End-point energy and half-life of the ^{187}Re β decay

M. Galeazzi,* F. Fontanelli, F. Gatti, and S. Vitale†
University of Genova and INFN, Via Dodecaneso 33, I-16146 Genova, Italy
(Received 13 December 1999; published 1 December 2000)

A high statistics measurement of the β decay of ^{187}Re with a cryogenic microcalorimeter has been performed. The high accuracy and the calorimetric nature of the measurement allow setting a value for the end-point energy of the decay in a metallic rhenium crystal equal to $[2470 \pm 1(\text{stat}) \pm 4(\text{syst})]$ eV. A good extrapolation of the spectrum to zero energy has also been possible thanks to the stable and well determined detector response down to the energy threshold of about 420 eV. This allows an estimate of the ^{187}Re half-life of $[4.12 \pm 0.02(\text{stat}) \pm 0.11(\text{syst})] \times 10^{10}$ yr. Both results are significantly better than the previous measurements reported in the literature.

DOI: 10.1103/PhysRevC.63.014302 PACS number(s): 23.40.−s, 21.10.Tg, 27.70.+q, 29.40.Wk

I. INTRODUCTION

The ^{187}Re β decay is characterized by the lowest known end-point energy and by a very long half-life, therefore its study has always been difficult. The number of experiments that studied ^{187}Re is limited as is their accuracy [1–4]. Current estimates of the end-point energy and of the half-life have a very pure accuracy and they often do not agree each other [3–6]. On the other end, due to its low end-point energy ^{187}Re is particularly suitable for a calorimetric experiment that measures all the energy released in the decay except that of the emitted neutrino. In order to obtain maximum performance in terms of detector response and efficiency, we used cryogenic microcalorimeters [7–9].

A good characterization of the ^{187}Re β decay is not only interesting by itself, but was also motivated by other considerations. The ^{187}Re isotope was proposed by our group [10] in 1985 as an alternative experiment to the study of the tritium β decay in order to evaluate the electron neutrino mass. Currently three groups (including ours) are working in parallel neutrino mass experiments using ^{187}Re [11–14], Since the experiments are based on the study of the β spectrum in the end-point region, a good knowledge of the end-point energy is a fundamental requirement. Moreover, the ^{187}Re half-life is evaluated to be of the order of the age of the Universe. This makes the isobaric pair ^{187}Re-^{187}Os an important nucleochronometer that can be used to provide terrestrial, Solar System, and cosmic chronologies [6], assuming that a good estimate of its half-life can be provided.

The β decay of ^{187}Re was observed for the first time using a cryogenic microcalorimeter in 1992 by this group [8,9]. After a few years spent improving the detector performance, the first high statistics calorimetric measurement has now been realized. About 6 000 000 ^{187}Re events in the energy range from 420 eV to the end point have been acquired with an energy resolution of about 41 eV RMS (see Fig. 1) [7]. The high statistics and good performances of the experiment allow the measurement of the physical quantities related to the ^{187}Re decay, the end-point energy and half-life, with an accuracy never obtained before. This is a necessary step in the understanding of the beta decay of ^{187}Re that could lead to a limit on the electron antineutrino mass in the near future.

Since this is the first high statistics measurement on ^{187}Re with cryogenic microcalorimeters, particular care has been used in the reduction of the data. Several behaviors could affect the spectral shape of the decay, influencing the experimental results. All the known behaviors have been considered and analyzed in detail. The detector characteristics turned out to be relatively simple and well understood. The experimental spectrum follows the expected distribution over the full energy range. This increases confidence in the interpretation of the data and strongly reduces the systematic errors of the experiments.

II. EXPERIMENTAL SETUP

A cryogenic microcalorimeter is composed of three parts, an absorber, which converts the energy of the incident radiation into heat, a sensor that detects the temperature variations of the absorber, and a weak thermal link between the detector and a heat sink [15,16]. The operating principle of a microcalorimeter is simple. When radiation is absorbed, its energy is eventually converted to thermal phonons and the temperature of the detector first rises and then returns to its

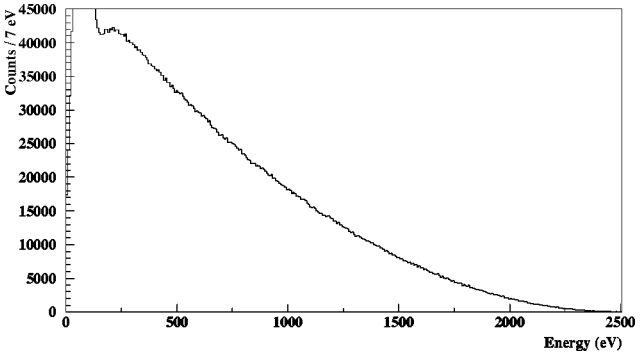

FIG. 1. High statistics spectrum of the ^{187}Re β decay acquired with a cryogenic microcalorimeter.

*Present address: University of Wisconsin, Physics Department, 1150 University Ave., Madison, WI 53706.
†Fax: +39 010310075. Electronic address: vitale@ge.infn.it

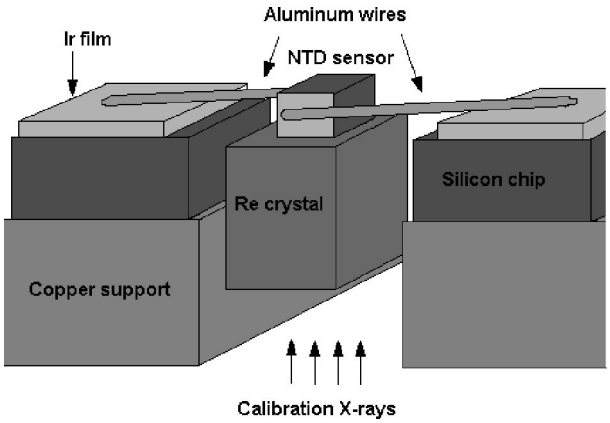

FIG. 2. Schematic of the microcalorimeter used. The connection to the heat sink is provided by an Ir film on a silicon chip where the aluminum wires are bounded. The silicon chip is glued to the refrigerator mixing chamber.

original value due to the weak thermal link with the heat sink. The temperature change is proportional to the energy of the incident radiation and is detected by the sensor. The sensor is generally a resistor whose resistance has a strong dependence on the temperature at the working point. Such a resistor can be biased either at constant current or at constant voltage, the temperature variation is thus read out respectively as voltage variation or current variation.

^{187}Re constitutes the 62.6% of natural rhenium, therefore a natural rhenium compound can be used instead of an isotopically enriched sample. In the experiment we used a rhenium single crystal of 1.572 mg as absorber, with an activity of about 1.1 Bq (see Sec. VI for details). This is a superconductor at the working temperature. The sensor is a neutron transmutation doped (NTD) germanium thermistor ($230\ \mu\text{m}\times 100\ \mu\text{m}\times 100\ \mu\text{m}$). Sensor and absorber are connected with a small drop of epoxy (Epotek H301-2) and the microcalorimeter is suspended by two ultrasonic bounded Al wires ($\Phi = 15\ \mu$m) that also provide the electrical connection and the weak thermal connection to the heat sink. A schematic of the microcalorimeter is reported in Fig. 2.

The use of a crystalline ^{187}Re source has already led, in a previous analysis, to the discovery of the influence of a crystalline structure on a β decay [17]. This phenomenon, named beta environmental fine structure (BEFS), was hypothesized in 1991 [18]. Its effect is an oscillatory modulation of the beta spectrum of the order of 1%, whose parameters depend on the crystalline structure. The details of the effect are reported in [17,19] and are taken into account in this analysis.

The heat sink for the microcalorimeter is provided by a ^{3}He-^{4}He dilution refrigerator which is able to maintain the mixing chamber at the working temperature of some tens of mK for an ''infinite'' time. During the measurement the refrigerator ran at the base temperature of 60 mK for uninterrupted periods up to two months.

The detector is shielded by a small piece of Roman lead to reduce the radioactive background. A small hole with a Be window is used for the x rays from the calibration source. The calibration source is a removable fluorescence source of Cl, Ca, and Va. The salts of the source are excited by an ^{55}Fe x-ray source that is also used for the calibration. The total count rate of the calibration source on the detector is about 1 Hz.

The fluorescence source can be removed through a mechanical control at the top of the refrigerator. When the fluorescence source is removed for high statistics measurements at low background, the calibration is provided by ^{55}Fe x rays (5898 eV and 6490 eV) with a count rate of about 10^{-3} Hz. The stability of the system has been tested and it has been proven to be very good over periods of days, so that such a low activity is sufficient for a good energy calibration.

III. THE DATA ACQUISITION

The microcalorimeter is biased at constant current. At every energy release in the microcalorimeter the temperature variation shows up as a voltage variation across the sensor. This signal, of the order of 10^{-5}–10^{-4} V is first read out using a low temperature JFET amplifier with low output impedance and unitary gain. Thus the signal can be read out using a low noise, high gain, ac amplifier at room temperature. The signal, now of the order of hundreds of mV, is amplified and filtered using a commercial amplifier. At this point the signal is split, part of it goes in the trigger channel, part of it goes directly to an analog to digital converter. After the digital conversion the data are stored on a disk and analyzed off line by software [20].

The low noise readout electronics is composed of a source follower with two matched JFETs in cascode configuration (for a complete description see [21]). This is cooled to about 150 K in a thermally shielded box in the inner vacuum chamber of the refrigerator. The output is forwarded to a noise-matched amplifier at room temperature. In the operating conditions, the overall voltage noise density ranges between 0.8 and 1.1 nV/$\sqrt{\text{Hz}}$ at 1 kHz. The $1/f$ noise contributes an excess noise less than 3 nV/$\sqrt{\text{Hz}}$ at 1 Hz.

The analog to digital converter is a commercial 12 bit CAMAC waveform recorder (LeCroy Model 6820). The instrument is set to record a file of 1024 12-bit data words at every trigger with a sampling rate of 5 kHz. The hardware discriminator level for the trigger is set to about 400 eV. The process is controlled by a digital VAX station 4000/60.

The amplitude of the pulses is determined by a digital optimum filter [22]. The filter consists in the cross correlation of each pulse with a reference pulse, with the maximum of the correlation taken as an estimate of the amplitude. In the data analysis only events with an energy above 420 eV have been considered to take into account possible variations of the trigger threshold during the months of data taking.

Generally the pulses have a very definite shape: a fast rise time (less then 1 ms) followed by a slow decay (a few tens of ms); this makes possible the use of pulse shape analysis: for every recorded pulse, the chi square function between the pulse and the normalized reference pulse is evaluated in order to reject spurious pulses, pulses with noise spikes superimposed and pileup not previously detected. For each pulse

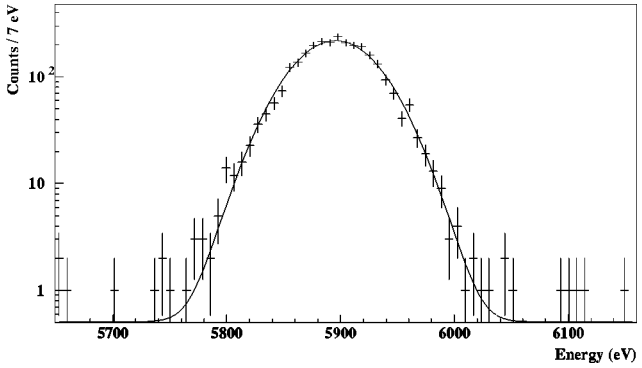

FIG. 3. ^{55}Fe K_α line in logarithmic scale, and Gaussian fit.

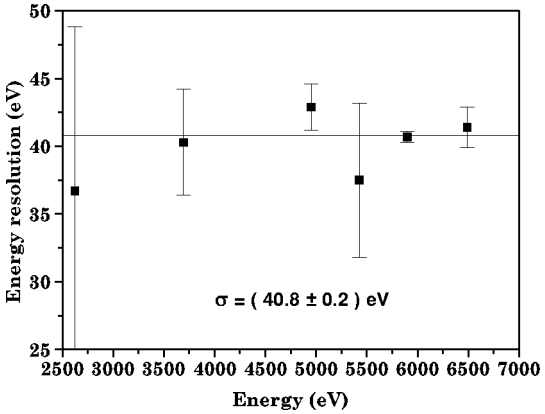

FIG. 4. Detector energy resolution versus energy.

the rise time, the decay time and the pretrigger slope and noise are also computed for a successive shape analysis using the software PAW [23].

IV. DETECTOR CHARACTERISTICS

The first step in the analysis of the data from the microcalorimeter is the investigation of the detector characteristics. In order to have good confidence in the physical results, all the known experimental behaviors that could affect the interpretation of the data have been analyzed in detail. These include the following: the detector function response; the detector energy resolution; the energy calibration and detector linearity; the effect of unidentified pileup; spectrum distortion due to electron escape; the effect of the energy interval on the fit; the effect of the data reduction and in particular of the cuts in the pulse shape analysis; the goodness of the theoretical spectral shape; and the confidence in the fit procedure.

Detector response. In general the resolution function of a microcalorimeter is Gaussian, but the presence of a small tail either toward low energies or toward high energies could affect the experimental results. Figure 3 reports, in logarithmic scale, a close view of the ^{55}Fe K_α line fitted with a Gaussian distribution. The energy response of the detector is in good agreement with a Gaussian distribution. Any low-energy or high-energy tail, if present, contributes to less than 0.1% to the total counts. The effect of such a possible tail on the ^{187}Re spectrum has been evaluated by Monte Carlo simulation and it is negligible with respect to the statistical uncertainties.

Detector energy resolution. In conventional detectors the energy resolution depends on the energy, while in microcalorimeters in general it does not, but such an effect must be investigated for a good interpretation of the data. In Fig. 4 the energy resolution σ of the microcalorimeter is reported as a function of the energy. The data have been fitted both with a constant and a linear function of the energy. The linear fit does not show any significant energy dependence, with a slope of $(-3.6\pm7.8)\times10^{-4}$, while the fit with the constant gives an energy resolution of

$$\sigma=(40.8\pm0.2)\ \text{eV}.$$

In order to see how a bad estimate of the energy resolution affects the experimental results, a series of fits scanning the energy resolution several eV around the expected value has also been performed and the results are reported in Sec. V.

Energy calibration. The measurement made with the fluorescence source shows a detector nonlinearity. This is well described by a parabolic distribution of the energy versus the pulse amplitude. The effect of the nonlinearity is about 0.5% for the ^{55}Fe K_α line and about 0.16% in the region of the end point. The high statistics measurement was performed without the fluorescence source, so that a long term change in the detector nonlinearity would not have been detected directly. Two considerations give good confidence that this is not a concern: the detector nonlinearity depends on the working conditions, which, with and without the fluorescence source, were exactly the same; and the energy nonlinearity in the high statistics measurement, evaluated using the two ^{55}Fe peaks and assuming that the calibration line passes through the origin, is in perfect agreement with the detector nonlinearity evaluated with the fluorescence source. The detector nonlinearity introduces a systematic error in the end-point energy evaluation which has been evaluated from the parabolic fit and has been included in the experimental results.

Unidentified pileup. To properly evaluate the undetected pileup that could affect the measurement, three different methods have been used. A Monte Carlo simulation to generate pulses in a format compatible with the analysis procedure has been made [20]. The simulation also keeps track of the original pulses generated. Therefore for a set of simulated data it is possible to check how correctly the analysis program reconstructs the original information. It is then possible to build a ''spectrum of pileup,'' composed of pulses classified as good pulses by the analysis program, while actually composed of more than one event. In particular, a set of 10 000 000 simulated events has been generated with the same characteristics as the microcalorimeter events. The spectrum of pileup is smoothed and added to the theoretical spectral shape in the fit procedure. An extra parameter which represents the ratio between the beta spectrum and the pileup is then introduced in the fit. The pileup spectrum has also been theoretically calculated. The theoretical calculation assumes an energy dependence of the pileup compatible with the experiment. The result of the theoretical calculation is in

good agreement with the spectrum of pileup obtained using the Monte Carlo simulation. The experimental results have also been compared with the results obtained using a second microcalorimeter, with smaller activity and different energy resolution, and therefore smaller influence of the pileup (the unidentified pileup in the second microcalorimeter is evaluated to be about 1/3 of that in the first one). The results from the two microcalorimeters are in perfect agreement, indicating that the evaluation of unidentified pileup does not introduce any systematic effect on the physical results of the experiment.

Energy distortion due to electron escape. The absorber is a rhenium crystal, then the radiation source is uniformly distributed in it. This means that if a β decay happens in a nucleus close enough to the surface of the crystal the emitted electron could escape from the surface, or could produce an x ray that escapes from the surface. This effect has been investigated and the conclusion has been that it affects a very thin layer near the surface of the crystal, equal to less than 0.01% of the total volume. The distortion introduced by the escape is therefore completely negligible with respect to the statistical uncertainties.

The data reduction. An important point that is the base for every analysis is ''how well the spectrum produced can be trusted.'' In particular, if some of the parameters of the pulse shape analysis are energy dependent, the cuts of the analysis could introduce an artificial distortion to the spectrum. The analysis has therefore been done avoiding most of the cuts that are generally included. This worsens a little the energy resolution of the detector, but strongly improves the confidence on the results. Only a light cut on the χ^2 parameter has been used in order to remove possible noise spikes or other experimental artifacts that could affect the measurement. Two spectra have been reduced using two different cuts, and the analysis has been performed on both. No systematic difference in the results has been found. Moreover the complete data reduction procedure has been repeated independently by two members of the team and the results do not show any evidence of a systematic difference between the two sets of data.

Confidence on the fit procedure. The program to perform the fit on the experimental data is relatively complicated. A small error in the software could pass undetected even to an accurate inspection. For this reason the fit procedure has been checked using Monte Carlo simulated data (see [20]). In addition two completely independent fit routines have been realized by two members of the team and the results obtained are in good agreement.

Theoretical spectral shape. In an experiment measuring the end-point energy and half-life of a β decay, the effect of the neutrino mass is negligible. In the approximation of an electron antineutrino with mass zero, the theoretical spectral shape of ^{187}Re can be represented as

$$N(E,Z) \propto F(Z,E) \cdot S(E) \cdot E \cdot p_e \cdot (Q-E)^2, \qquad (1)$$

where E is the calorimetric energy of the decay (i.e., the energy of the emitted electron, plus the energy of the final excited states), Z is the number of protons in the original nucleus, $F(Z,E)$ and $S(E)$ are, respectively, the Fermi function and the shape factor of the decay, p_e is the momentum of the emitted electron, and Q is the end-point energy. The term $F(Z,E) \cdot S(E) \cdot E \cdot p_e$ has been theoretically calculated by Büring [24]. This is almost constant and changes less than 5% in the whole energy interval. A detailed explanation of how the expression is obtained and of the influence of the different terms can be found in [7,20].

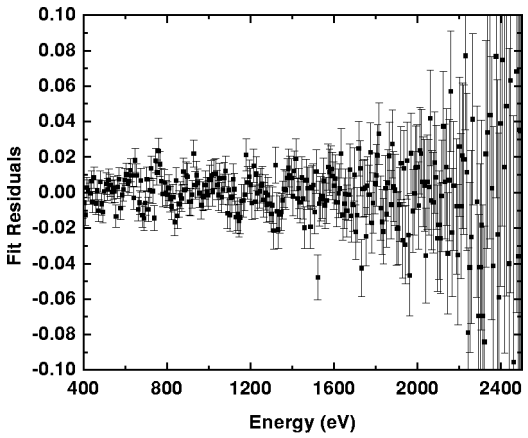

FIG. 5. Residuals of the best fit of the experimental spectrum with the theoretical distribution.

The theoretical calculation has been compared with the experimental spectrum from 420 eV to the end-point energy and the result shows good agreement between the two. The residuals of the fit are reported in Fig. 5. Of particular interest for the calculation of the half-life of the decay is the goodness of the theoretical calculation below the energy threshold of 420 eV. In this regard, a second microcalorimeter, with a similar geometry to the one used for the high statistics measurement, has been built. In this microcalorimeter the absorber consists of a rhenium polycrystalline foil 230 μm$\times$100 μm$\times$100 μm. The activity of this microcalorimeter is very small (0.06 Bq), thus it is unsuitable for a high statistics measurement in the end-point region, but the energy resolution is 13 eV RMS and the energy threshold about 60 eV. It has therefore been possible to check the goodness of the theoretical distribution from 60 eV to 500 eV. The spectrum is in agreement with the theoretical distribution with an accuracy better than 0.1% in this energy interval, giving good confidence in the extension of the experimental spectrum to zero energy.

V. THE ^{187}Re END-POINT ENERGY

Having good confidence in the reduced data it is possible to analyze them for the determination of the end-point energy. In order to evaluate the parameters of the β distribution, the experimental spectrum is fitted with the expected distribution which includes the theoretical β spectrum, a flat background, and the unidentified pileup distribution. This distribution is convoluted with the detector response which is a Gaussian with width 40.8 eV independent of the energy.

Following the recommendations of the Particle Data Group (PDG) [25] for the estimate of the parameters we

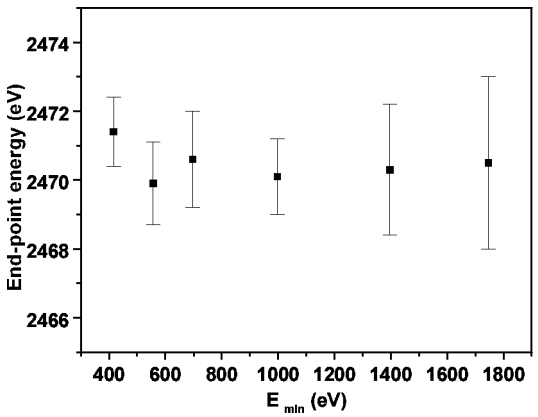

FIG. 6. Dependence of the end-point energy on the lower limit of the energy interval for the fit.

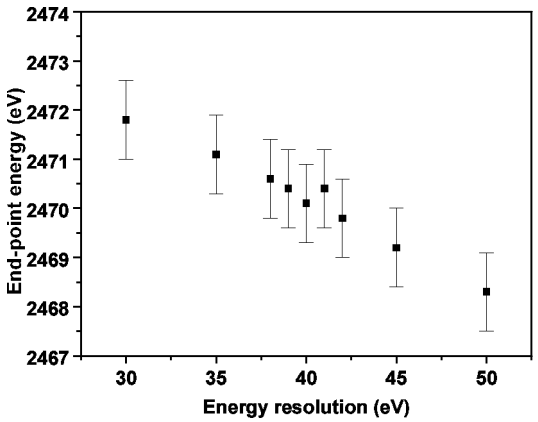

FIG. 7. Dependence of the end-point energy on the detector energy resolution assumed in the fit.

utilized the *Maximum Likelihood* method, which has already been treated in detail by many authors [25]. To search for the best fit we use the program MINUIT [26] of the Laboratoire Européen pour la Physique des Particules (CERN); to evaluate the errors we followed [27,25], and for the confidence intervals evaluation we utilize the ordering principle proposed by Feldman and Cousins [28] and accepted by the PDG [25], which allows the separation between the confidence interval C.L. and the goodness of fit C.L. For the goodness-of-fit calculation a χ^2 test is also implemented.

The parameters that are free in the fit are the end-point energy Q, the amplitude of a flat the background B, and the relative amplitude of the unidentified pileup P. The total amplitude of the distribution has been calculated normalizing the integrals of the theoretical and experimental distributions. The effect of distortions in the background with respect to a flat distribution is negligible, since in the energy range of interest the background is always a negligible term, dominated by the spectrum and by the pileup.

For the evaluation of the end-point energy the effect of the BEFS has not been included in the fit, since we verified that its average in the full energy range is zero, and therefore it affects neither the calculation of the end-point energy, nor that of the half-life. The upper limit of the fitting interval has been varied between 2650 eV and 2800 eV, without any change in the value of the end-point energy. The lower limit of the fitting interval has been varied between 420 eV and 1750 eV. The end-point energy as a function of the lower limit is reported in Fig. 6. The statistical error is about 1 eV and the results are stable in the full energy range. The error due to the choice of the energy interval is smaller than 1 eV. The convergence of the fit routine is good in the full interval and the reduced χ^2 function is about 1 in the full range ($\chi^2=257$ with 257 degrees of freedom for the energy range 1000–2800 eV, with similar results in the other ranges), indicating a very good agreement between experimental data and theoretical distribution. It is a remarkable result that the shape of the spectrum is stable and in agreement with the theoretical prediction over such a wide energy range, considering that in the experiments with tritium only a small fraction of the spectrum is not distorted.

The dependence of the end-point energy on the assumed energy resolution has also been investigated. In the energy interval 420–2800 eV the experimental spectrum has been fitted varying the energy resolution between 30 and 50 eV, and the results are reported in Fig. 7. As expected from trivial considerations, the end-point energy decreases when the energy resolution is increased, but the dependence is very slow: the end-point energy varies about 1 eV when the energy resolution σ is varied by 5 eV.

The effect of the unidentified pileup has been investigated too. The total unidentified pileup resulting from the fit is $P=0.0628\pm0.0017$. Changing the shape of the unidentified pileup does not affect appreciably the calculation of the end-point energy. Even using the drastic assumption of a flat pileup spectrum the end-point energy changes of only 2 eV.

From the previous considerations it is possible to set the end-point energy of the ^{187}Re β decay equal to

$$Q=[2470\pm1(\text{stat})\pm4(\text{syst})]\ \text{eV},$$

where the systematic error is due to the influence of the energy nonlinearity, as mentioned before, plus the choice of the energy interval.

VI. THE ^{187}Re HALF-LIFE

The determination of the ^{187}Re half-life was possible thanks to the very pure rhenium sample. Since the characteristics of the sample are known, the total number of radioactive nuclei is a known quantity. Thus measuring the total activity of the sample (extrapolating the β spectrum to zero) it is possible to calculate the half-life of the isotope. In the case of ^{187}Re the relation that links the activity of the sample to the half-life is

$$\tau_{1/2}=\frac{\ln 2\cdot N\cdot m\cdot f\cdot F}{A\cdot CR}, \tag{2}$$

where N is the Avogadro number, m is the mass of the crystal, f is the relative amount of radioactive nuclei in the sample, F is the factor that takes into account the extension to zero of the spectrum, A is the atomic mass, and CR is the

measured count rate of the sample above threshold. The value of F depends on the energy threshold of the detector, on the end-point energy, and on the theoretical spectral shape at very low energy; the other parameters are known or measured quantities.

The measurement of the ^{187}Re half-life has been done in two days of data taking with a special setup for the evaluation of the dead time. The trigger channel has been connected to a counter unit in order to count the total number of triggers coming from the trigger circuit plus the number of triggers coming from the trigger system happening during the dead time of the A/D converter. Since the dead time of the trigger circuit is negligible, this allows us to quantify with good accuracy the dead time of the A/D converter, equal to $(8.571 \pm 0.073)\%$. Data have been acquired in this configuration for a total real time $t = (164124 \pm 20)$ s.

The data have been analyzed without cuts in the pulse shape routine. Other factors that have been included in the calculation of the half-life are the following.

The ''dead time'' of the analysis. When the trigger algorithm finds more than two pulses in a waveform, it discards the waveform. The analysis program keep track of the number of pulses identified and of the number of pulses discarded so that it is possible to correct the count rate. This software dead time is equal to $(3.09 \pm 0.26)\%$.

Double pulses. Whenever the program finds two pulses in the same waveform it is able to separate the two and analyze them independently, so that the pulses are not lost. The goodness of the procedure has already been reported in a previous paper [20]. The contribution of such events corresponds to $(29.99 \pm 0.24)\%$ of the total counts.

Pileup events. The unidentified pileup events are in principle counted as single event instead of double. To correct for that we used the result of the fit routine used for the end-point energy determination. As described in Sec. V, one of the fit parameters is in fact the ratio P between the unidentified pileup and the total number of counts, equal to 0.0628 ± 0.0017.

Two different energy thresholds (350 eV and 500 eV) have been used to calculate the detector count rate. This allows one to avoid any possible effect of low energy spurious noise. The total count rate measured above 350 eV, when the previously described effects are taken into account, is 1.112 ± 0.006 Hz. The count rate above 500 eV is 0.912 ± 0.005 Hz. The two count rates are in perfect agreement with the expected distribution.

As already reported in Sec. IV, the theoretical expression has been experimentally tested from 60 eV to the end point; but the its goodness below 60 eV is unknown. An absolute systematic error has been therefore estimated considering two extreme possibilities: the upper limit in the number of counts below 60 eV comes from an extension to zero energy which follows the almost quadratic distribution of higher energies, while the lower limit comes from a distribution that goes rapidly to zero below the energy of 60 eV.

The half-life which is obtained in this way is

$$\tau_{1/2} = [4.12 \pm 0.02(\text{stat}) \pm 0.11(\text{syst})] \times 10^{10} \text{ yr}.$$

This result is in agreement with the previous measurements made with geochemical and mass spectrometer experiments [6,29,30] and it is, at the status of the art, the best estimate of the ^{187}Re half-life.

VII. CONCLUSIONS

The study of the β decay of ^{187}Re has always been difficult. The measurement of the decay main parameters, the end-point energy and the half-life of the decay, have therefore been affected by large uncertainties. Using a cryogenic microcalorimeter we have been able to measure such parameters with good accuracy. The simple and well understood detector characteristics made the interpretation of the data relatively simple, increasing the confidence in the experimental results and reducing the systematic errors. This is very promising for the next step of the experiment which is the determination of the electron antineutrino mass value.

ACKNOWLEDGMENTS

We would like to thank our collaborators at the University of Genova for the helpful discussions and suggestions, Professor W. Bühring for his fundamental contribution in the theoretical calculation of the β spectral shape, and Professor E. Fiorini for supplying the Roman lead for the detector shielding. This work was supported by INFN and by the European Union, Research Network Contract No. FMRXCT98-0167 (DG12-MIHT) ''Cryogenic Detectors.''

[1] S. Naldrett and F. Libby, Phys. Rev. **73**, 487 (1948).
[2] C. J. Wolf and W. H. Johnston, Phys. Rev. **125**, 307 (1962).
[3] R. L. Brodzinski and D. C. Conway, Phys. Rev. **138**, B1368 (1965).
[4] E. Huster and H. Verbeek, Z. Phys. **203**, 435 (1967).
[5] M. Galeazzi, Nucl. Phys. B (Proc. Suppl.) **66**, 203 (1998).
[6] M. Lindner, D. A. Leich, R. J. Borg, G. P. Russ, J. M. Bazan, D. S. Simons, and A. R. Date, Nature (London) **320**, 246 (1986).
[7] M. Galeazzi, Ph.D. thesis, University of Genova, Italy, 1999.
[8] E. Cosulich, F. Fontanelli, G. Gallinaro, F. Gatti, A. M. Swift, and S. Vitale, Nucl. Phys. **A592**, 59 (1995).
[9] F. Gatti, Ph.D. thesis, University of Genova, Italy, 1992.
[10] S. Vitale *et al.*, Istituto Nazionale di Fisica Nucleare Report No. INFN/BE-85/02, 1985.
[11] E. Fiorini, Nucl. Instrum. Methods Phys. Res. A **444**, 65 (2000).
[12] A. Nucciotti *et al.*, Nucl. Instrum. Methods Phys. Res. A **444**, 77 (2000).
[13] F. Gatti, F. Fontanelli, M. Galeazzi, and S. Vitale, Nucl. Instrum. Methods Phys. Res. A **444**, 88 (2000).
[14] M. R. Gomes, T. A. Girard, C. Oliveira, V. Jeudy, and D. Limagne, Nucl. Instrum. Methods Phys. Res. A **444**, 84 (2000).
[15] M. Galeazzi, D. McCammon, and W. T. Sanders, in *X-Ray*

and Inner-Shell Processes, edited by R. W. Dunford, D. S. Gemmel, E. P. Kanter, B. Krässig, S. H. Southworth, and L. Young, AIP Conf. Proc. No. 506 (AIP, Melville, NY, 2000), p. 638.
[16] N. Booth, B. Cabrera, and E. Fiorini, Annu. Rev. Nucl. Part. Sci. **46**, 471 (1996).
[17] F. Gatti, F. Fontanelli, M. Galeazzi, A. M. Swift, and S. Vitale, Nature (London) **397**, 137 (1999).
[18] S. E. Koonin, Nature (London) **354**, 468 (1991).
[19] A. M. Swift, Istituto Nazionale di Fisica Nucleare Report No. INFN/BE-97/02, 1997.
[20] F. Fontanelli, M. Galeazzi, F. Gatti, A. M. Swift, and S. Vitale, Nucl. Instrum. Methods Phys. Res. A **421**, 464 (1999).
[21] F. Gatti and L. Parodi, Nucl. Instrum. Methods Phys. Res. A **444**, 129 (2000).
[22] E. Cosulich and F. Gatti, Nucl. Instrum. Methods Phys. Res. A **321**, 211 (1992).
[23] PAW (Physical Analysis Workstation), CERN Program Library entry Q121, Geneva, Switzerland, 1995.
[24] W. Büring, University of Heidelberg (private communication).
[25] Particle Data Group, C. Caso *et al.*, Eur. Phys. J. C **3**, 1 (1998).
[26] F. James and M. Roos, MINUIT Function Minimization and Error Analysis, CERN Library D506.
[27] F. James, Comput. Phys. Commun. **20**, 29 (1980).
[28] G. J. Feldman and R. D. Cousins, Phys. Rev. D **57**, 3873 (1998).
[29] J. M. Luck and C. J. Allègre, Nature (London) **302**, 130 (1983).
[30] J. M. Luck, J. L. Birck, and C. J. Allègre, Nature (London) **283**, 256 (1980).